Acta Geodyn. Geomater., Vol. 8, No. 2 (162), 169–187, 2011

VISUALIZATION OF THE FAULT SLIP CONNECTED WITH THE WEST BOHEMIA EARTHQUAKE SWARMS

Petr KOLÁŘ *, Bohuslav RŮŽEK,
Alena BOUŠKOVÁ and Josef HORÁLEK

Institute of Geophysics, Academy of Sciences of the Czech Republic, Boční II 1401, 141 31 Prague 4, Czech Republic
**Corresponding author's e-mail:* kolar@ig.cas.cz

(*Received* May 2011*, accepted* June 2011)

ABSTRACT

The West Bohemia earthquake swarm foci are approximated by a circular seismic source model, which radius is assumed to depend only on magnitude of the event. We consider two different models of average slip (i) a constant slip and (ii) a slip exponentially scaled to the magnitude of the event. Based on these assumptions, we stacked the contributions of individual events into representative final fault slip. We processed in such a way four significant swarms recorded during the last three decades in 1986, 1997, 2000 and 2008. Constant slip model indicates final slip was composed of 2 or 3 principal asperities located on one or two different planes. On the contrary, scaled slip model indicates that one big asperity prevails. It is not possible yet to select the preferred slip model. Analysis of the temporal activity of all swarms generally shows three principal phases: starting phase, main phase and fading phase; the upwards trend of activity spreading was observed (slip animation is presented in www supplement http://www.ig.cas.cz/kolar/StopPhase/Asperity). The maximal possible cumulative slip value may have reached the order of meters.

KEYWORDS: West Bohemia earthquake swarm, fault slip, fault dynamics, asperity

1. INTRODUCTION

Seismic activity in the West Bohemia (WB) region is the dominant seismic activity on the territory of the Czech Republic – see Figure 1. This activity is characterized by the repeated occurrence of the earthquakes swarms. The swarm in 1985/86 gave an impulse to start modern instrumental seismological observations (i.e., digital seismogram recordings). Four swarms, which are subject of this study, were of significant intensity (in years 1985/86, 1997, 2000 and 2008 respectively). The region is continuously monitored by the WEBNET seismic network (Horálek et al., 2000a; wwwWEBNET, 2010) and the activity has been subject to intensive studies (e.g., Stud. Geophys. et Geod., 2000, 2008 and 2009).

In our present work we try to understand a seismic swarm (i.e., a group of events allied in time and space) as one large earthquake with heterogeneous slip distribution (places with maximal slip we then call asperities). Such an insight can contribute to establish a general quantitative dynamic model of the swarm-like earthquake phenomenon.

2. METHOD

For modelling, we assume a circular model of seismic source and we estimate its radius using magnitude formula derived by Fischer and Horálek (2005):

$$r_s = 12 * 10^{0.33Ml}, \qquad (1a)$$

in which r_s is the source radius and Ml is the magnitude. Since eq. (1a) is of empirical nature, other nearly equivalent form is also valid:

$$r_s = 30 * 10^{0.35Ml}, \qquad (1b)$$

(Fischer, personal communication, 2010). Source radii computed by using formula (1b) correspond well to radii obtained from the inversions based on "Stopping phases" method (Kolář, 2011). The stopping phases method was designed by Imanishi and Takeo (1998, 2002).

Radially symmetric slip distribution s_{aver} can be approximated according to Keilis-Borok (1959) in form of

$$s_{aver} = K_1 \left(r_s^2 - r^2 \right)^{1/2}, \qquad (2)$$

in which r_s is the source radius and r is the distance from the source centre, and K_1 is a constant. In order to characterize the overall earthquake process, we sum individual slips produced by each event during the

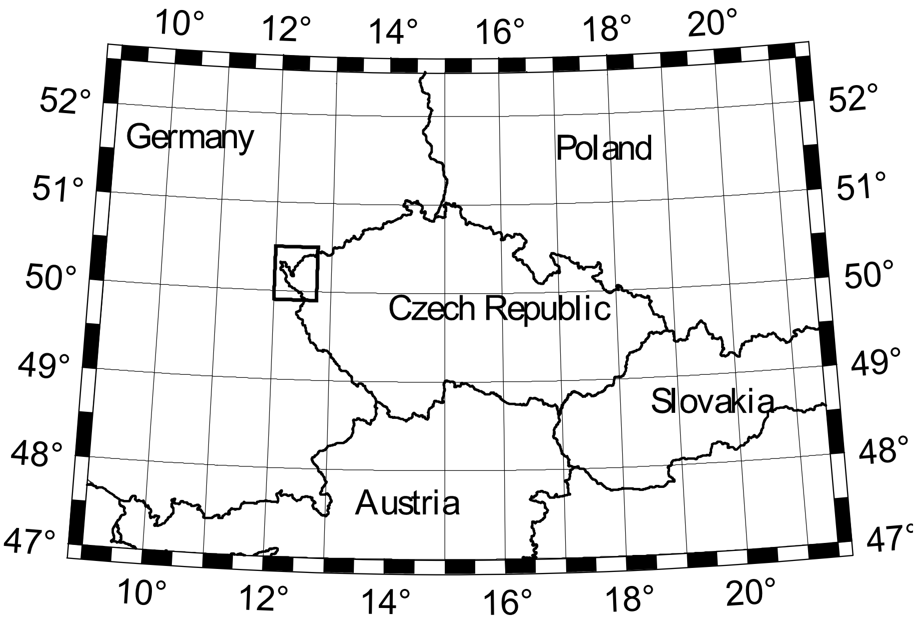

Fig. 1a Position of the West Bohemia region in Central Europe (marked by a square).

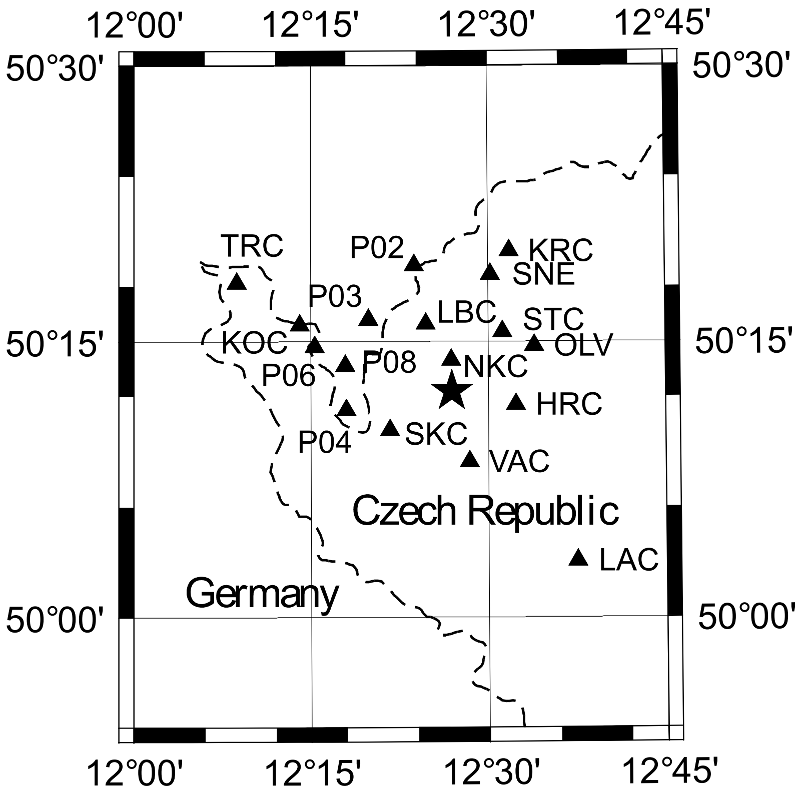

Fig. 1b Map of West Bohemia earthquake region, stations of WEBNET network (triangles) configuration during 2000 earthquake swarm and the swarm epicentre (asterisk). The more detailed maps or information are available at Epicentre map (2010).

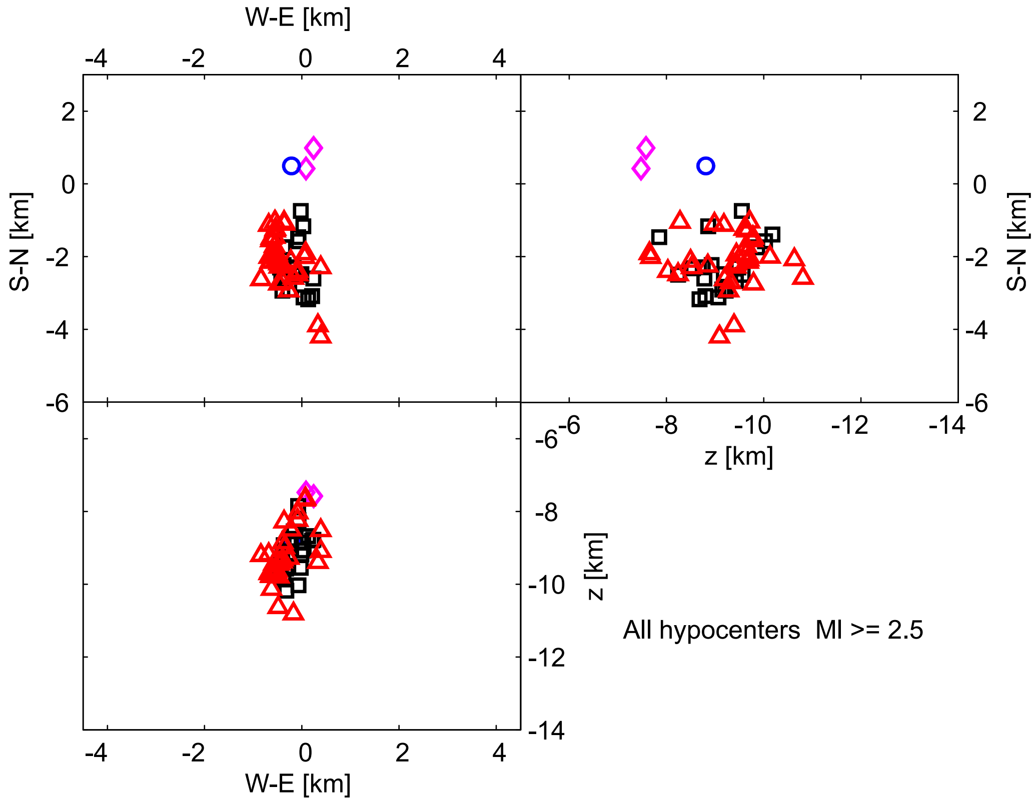

Fig. 1c Hypocentres of four considered swarms; horizontal projection (in NS-EW orientation) – upper left part; vertical projection into NS-z plane, view from E – upper right part; vertical projection in EW-z plane, view from S - lower left part. Distances are given in [km]; origin is in station Nový Kostel (NKC, N50.2331 E12.4479, alt. 564m). Not to make the figure to messy with respect of used scale, only events with magnitude Ml > 2.5 are plotted here. Figure shows that even if the swarms occurred in the same region, their locations are not identical and therefore the observed asperities cannot be identified with the same particular area/volume.

whole swarm. For our approximation we consider two models of average slip: (i) a constant average slip, which also represents a standard approach in many other works dealing with modelling of large earthquakes (in such a case a swarm is understood as one large meta-event with slow rupture which is manifested in form of single swarm sub-events) and, (ii) a scaled average slip for each event according to formula

$$s_{aver} = \frac{1}{30^2 \mu\pi} 10^{(0.35Ml+11.3)} \approx K_2\, 10^{(0.35Ml+11.3)} . \qquad (3)$$

In opposite to the first slip model, now the swarms are understood rather as a series of individual independent events, despite their concentration in time and space. Relation (3) is based on formula (1b), applying the well known relation between seismic moment M_0 and magnitude Ml (Hanks and Kanamori, 1979)

$$\log M_0 = 1.5Ml + 16.1 , \qquad (4a)$$

in which the values of coefficients are suited for large earthquakes. For the West Bohemia region with smaller events the coefficients are modified to values given by Hainzl and Fischer (2002)

$$\log M_0 = 1.05Ml + 11.3 \quad . \qquad (4b)$$

Note that the modification is not as dramatic as it may look since the seismic moment in eq. (4a) is given in [dyn cm] compared to [N m] in case of (4b). Seismic moment M_0 and average slip are connected by the formula

$$M_0 = \mu\, s_{aver}\, A , \qquad (5)$$

in which μ is a shear modulus and A is the source area, i.e., $A = \pi r_s^2$ in the case of circular source. All constants (K_i and μ) can be equal to one if only relative results are required. We will show later that numerical tests prove that alternatives for relation (3) significantly affect the inferred total slip pattern.

The summation of individual swarm event contributions is performed on projection planes (a horizontal one and two vertical ones, oriented in

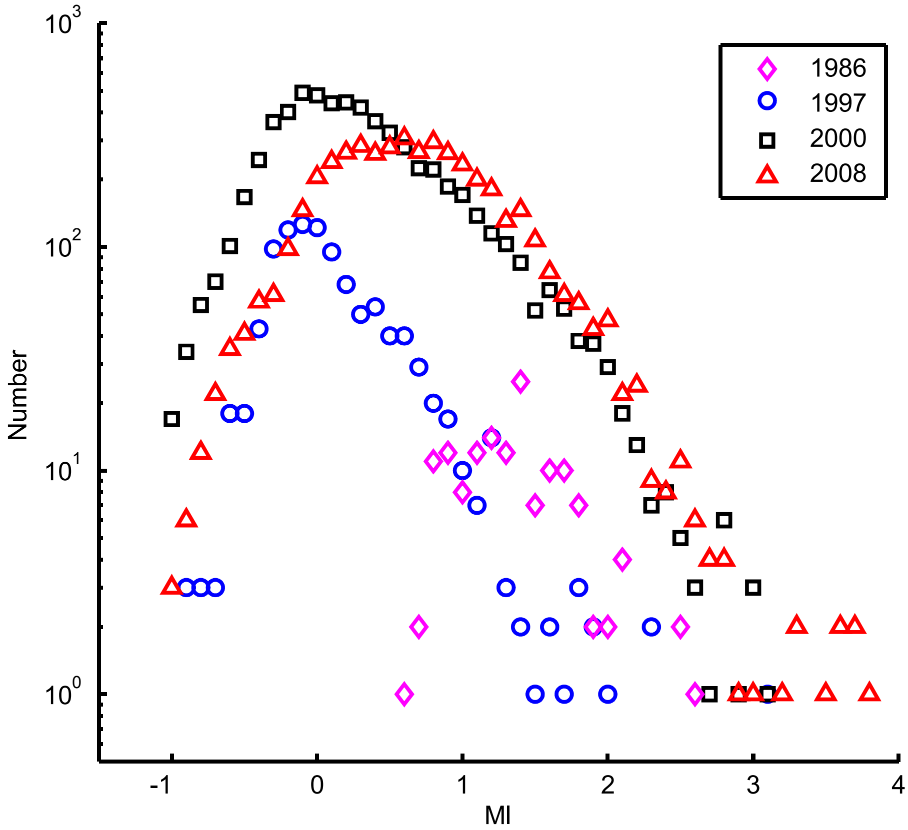

Fig. 2 Numbers of events versus magnitude for swarms 1986 (diamonds), 1997 (circles), 2000 (squares) and 2008 (triangles) are plotted; symbols are the same as in Fig. 1c. Figure gives information about data quality and values $Ml_{compl.}$ (given in Table 1) were estimated from it.

East-West and North-South directions). Individual finite sources with corresponding slips are projected into plane(s) and projected slips are summed on a dense rectangular grid (5 m grid spacing was used). Hypocenters are located using a "Master event" method (Fischer, personal communication, 2010); if a Master event location is not available, we use a standard bulletin location.

If the source mechanism of particular event is known, then the circular source of that orientation is projected onto considered projection planes (generally as an ellipse). Simultaneously, the slip value is proportionally contracted also, i.e., the slip vector is decomposed into its components laying in the projection planes. If source mechanism is not available, then the event is represented as a circular source with modelled slip at any projection plane.

Temporal-spatial behaviours of slipped areas are then studied.

3. DATA

For our study standard WEBNET catalogue data (wwwWEBNET, 2010) there were used (only well-located events were selected). Since there were processed data from period of almost three decades, the data set is inhomogeneous due to many changes of the recording equipment, geometry of the network, etc. Basic characteristics of the processed swarms are given in Table 1. We processed all four pronounced swarms that occurred since digital observation period has started, namely the swarms in years 1986, 1997, 2000 and 2008.

Particular swarms' characteristics are as follows:

The swarm 1986 represents the second part of a double swarm in 1985/86. Both analogue and digital instrumentations were operated in the region in course of 1985/86 swarm. Unfortunately, the quality of the data from 1985 is not sufficient for this study. Moreover, the catalogue of the 1986 swarm is incomplete. Despite this we processed all available data - 143 located events (Kolář and Vavryčuk, 1990; Fischer, personal communication, 2010), using magnitudes given by Neunhöfer (1988).

Swarm 1997 was recorded fully in digital form, which means significant increase of data quality. 70 source mechanisms are available for the swarm, which

Table 1 Basic characteristic of investigated swarms.

Swarm	duration [days]	number of events	Ml min.	R min [m]	Ml max	R max [m]	Ml compl. (estim.)	Ml total	R total [m]	num. of mech.	relat energy of mech [%]	max. slip without mech. [m]	max. slip with mech. [m]
1986	35	142	0.6	49	2.6	242	1.3	3.11	368	0	0	2.8	-
1997	45	1010	-0.9	15	3.1	365	0.0	3.18	391	70	94	7.7	1.5
2000	126	6271	-1.0	13	3.1	365	0.0	3.85	669	133	70	14.0	4.7
2008	143	4524	-1.0	13	3.8	641	0.6	4.30	957	99	31	40.4	25.1

Number of events represents number of processed events (not the total number of observed swarm events). Circular source radii $R_{min/max/total}$ are determined by formula (1b) with respect to the magnitude range of processed events. Magnitude of completeness Ml_{compl} is estimated from Fig. 2. Magnitude Ml_{total} (and corresponding source radius R_{total}) is determined in such a way, that energy of events is estimated using the standard Gutenberg-Richter magnitude-energy relation (6). The energy of events is summed and then total magnitude is evaluated with the use of inverted formula (6).

There are given numbers of know source mechanisms for each swarm, relative energy of events with known mechanism (estimated again with use of (6)) and estimated maximal slip without and with consideration of source mechanism influence.

represents more than 90% of released energy (Horálek et al., 2000b). The estimation of the released energy is based on the standard Gutenberg-Richter relation

$$\log E = 1.5Ml + 11.8 \quad . \tag{6}$$

The swarm 2000 data had already been completely processed, i.e., the final catalogue was available. 133 source mechanisms are available (Fischer and Horálek, 2005), which represent about 70 % of released energy.

Swarm 2008 was the largest one in the digital period of observation. The catalogue had not yet been fully finalized when we prepared this study. For this reason, results concerning the swarm 2008 can slightly change due to the ongoing detailed manual re-interpretation, namely of weak events having magnitudes in the range from -1 to 0. This effect is also documented in Figure 2. At the time of this study preparation there were available 99 source mechanisms (Vavryčuk, 2011), which represents about 30% of totally released energy, but there is a possibility that the number of determined source mechanisms could be finally several times higher.

4. RESULTS

4.1. FINAL SWARM SLIP PATTERNS

Final swarm slips are presented in Figures 3 – 6. For constant slip model usually 2 or 3 (exact number is rather subjective) most slipped areas can be found in each swarm. We call these areas "asperities". If slip scaled according to formula (3) the final pattern is more controlled by the strongest event in the swarm. The hypocentres are distributed approximately on a NS oriented vertical plane, possibly tilting to the E at the top. This fact is in general agreement with the study of swarm foci distribution.

The basic features of the swarm 1986 (Fig. 3) can bee seen despite of data incompleteness.

The image of the swarm in 1997 (Fig. 4) was rather messy, however, if vertical projection planes were rotated by 30^o clockwise, the situation became clearer. For constant slip we have again two asperities, this time situated on two approximately perpendicular vertical planes. This fact is also in agreement with the distribution of the swarm foci. This effect vanished for the scaled slip model. Note, that the swarm in 1997 was located in a relatively small area/volume.

The results for the swarm in 2000 and 2008 are in Figs. 5 and 6, respectively.

With use of formula (3) we tried to bind the final relative displacement to the absolute values, the calculated values are given in Table 1 (value of shear modulus $\mu = 1*10^{11}$ [N/m^2] was used). It follows from the table that when source mechanisms considered, the value of the estimated maximal slip decreases several times. This is the consequence of the slip vector decomposition into planes of projection, which cannot be done, when the source mechanism is not available and we had to adopted directionless simplification. Our estimation is based on simplifications and the presented values are summed projection of all considered events which are in reality distributed in a volume. Nevertheless, it seems that maximal displacement in certain small area or volume respectively, could reach order of meters for the processed swarms.

4.2. DYNAMIC SWARM SLIP PATTERNS

In addition to the above mentioned final swarm slips, we also studied slip development in time. We divided each swarm into several sub-periods (10-16) in such a way that each period contained an individual swarm phase, which can be seen in daily number of events versus time diagram – Figure 7; the more standard distribution – Ml versus time – is given for comparison in Figure 8. We calculated the slip for each of these sub-periods. The results are given in Figure 9 (an example with constant slip model), and in a more figurative way and for both slip models also as movie animations on ASPERITIES (2010) www pages.

It follows from the appropriate figures (and animations) that course of each swarm can be roughly characterized by three stages: (i) **Starting period**, which is characterized by random distribution of small events. (ii) **Main period**, which involves essential amount of slip generation and consequently also dominant energy release; two or three fundamental asperities (if constant slip model considered) are generated. There was not observed any simple rule for the temporal-spatial development of the slip pattern but general upward movement of the seismicity is common. (iii) **Fading period,** which is generally characterized by the occurrence of weak events distributed along the whole seismoactive fault area.

Note, that the swarm 2000 started rather abruptly (c.f. Figs. 7c and 8c) and the existence of its starting period is more subdued.

5. CONCLUSIONS

Presented work is based on several simplifications:

- circular earthquake source model is supposed
- the source radius is only a function of the event magnitude - see formula (1)
- we implicitly suppose a constant stress drop
- if source mechanism is not known, its influence is neglected; the prevailing alignment of events onto a plane, or several planes respectively, during the swarm course is not accounted for
- in this case, we summed only the magnitude of the displacement irrespective of its vector nature

The final slip projected onto (three) planes is observed under the assumption of two simplified models of an event's average slip. As it follows from the presented figures, final swarm slip pattern depends

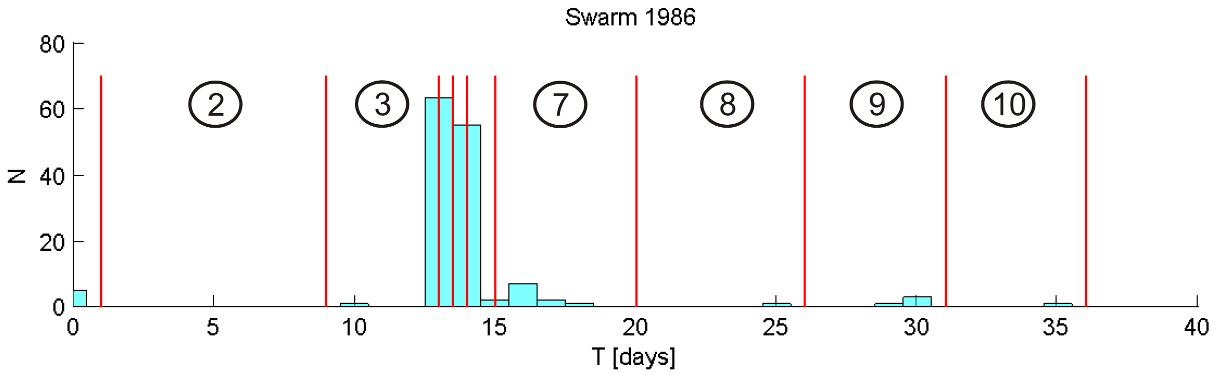

Fig. 7a

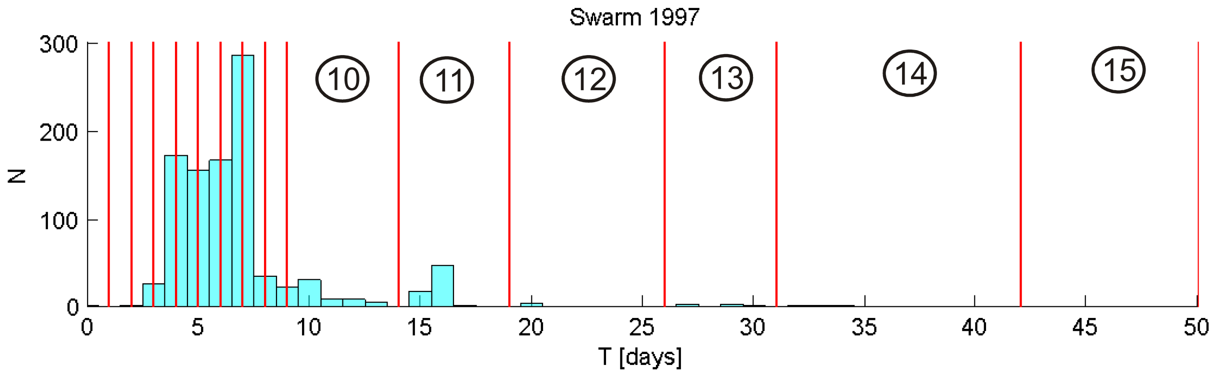

Fig. 7b

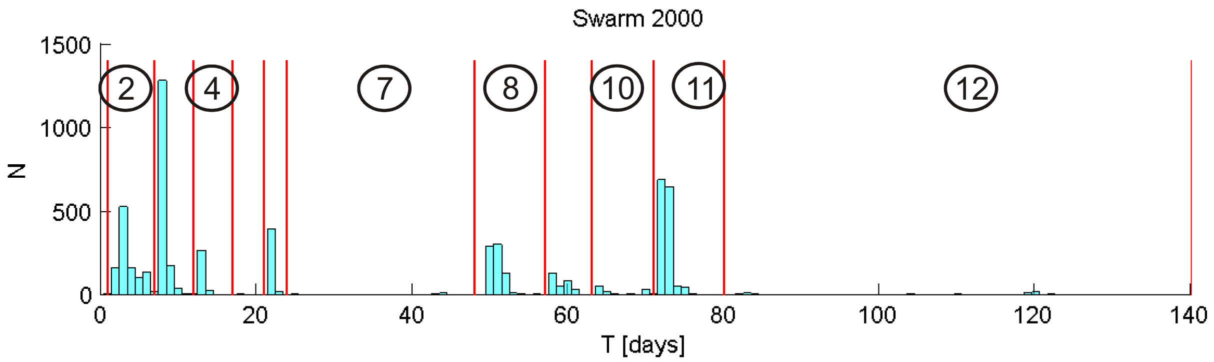

Fig. 7c

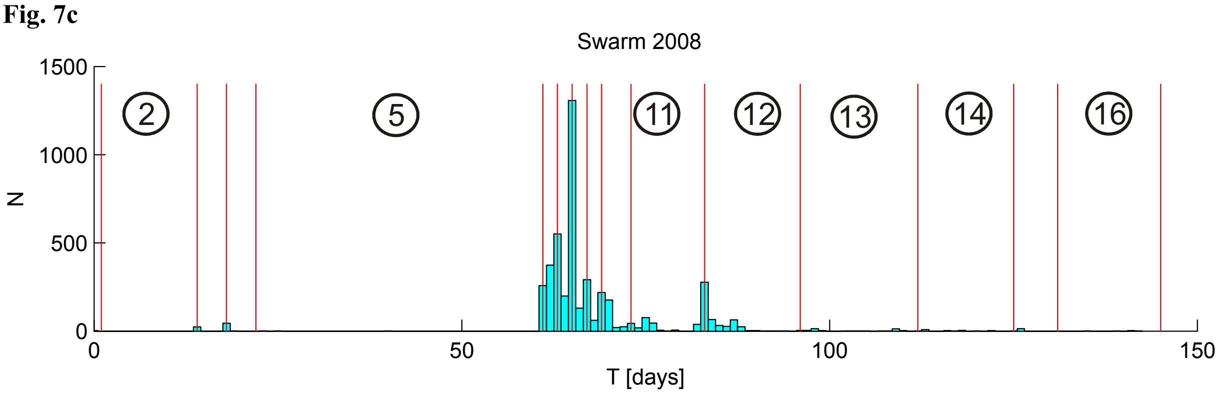

Fig. 7d

Fig. 7 Swarms division into time series. The columns represents daily number of events (magnitude of particular events is not considered), the vertical lines separate individual time interval (larger time intervals are numbered for more comfortable orientation in Figure 9 – see below). Fig. 7a – 1986; Fig. 7b – 1997; Fig. 7c - 2000 and Fig. 7d - 2008.

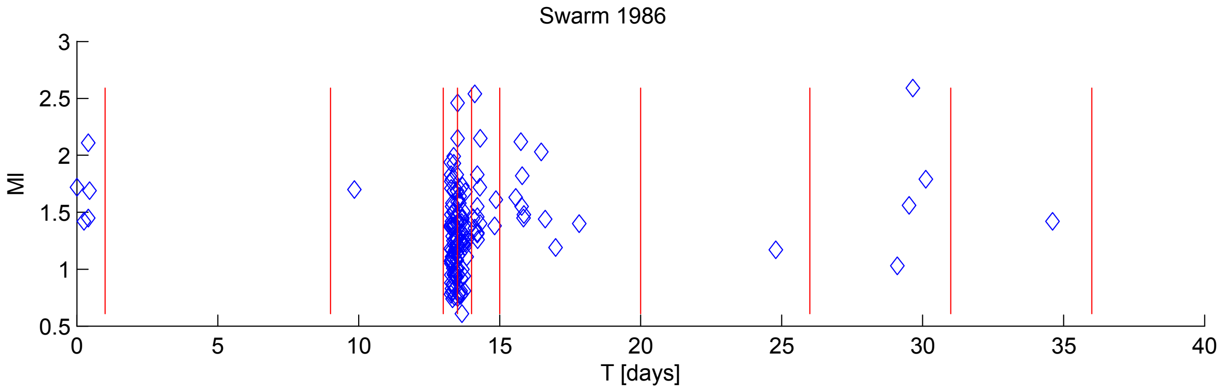

Fig. 8a

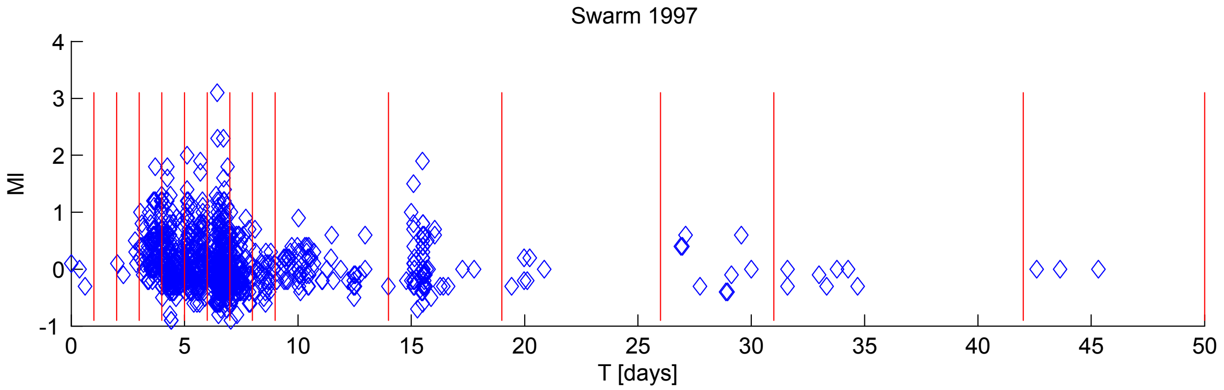

Fig. 8b

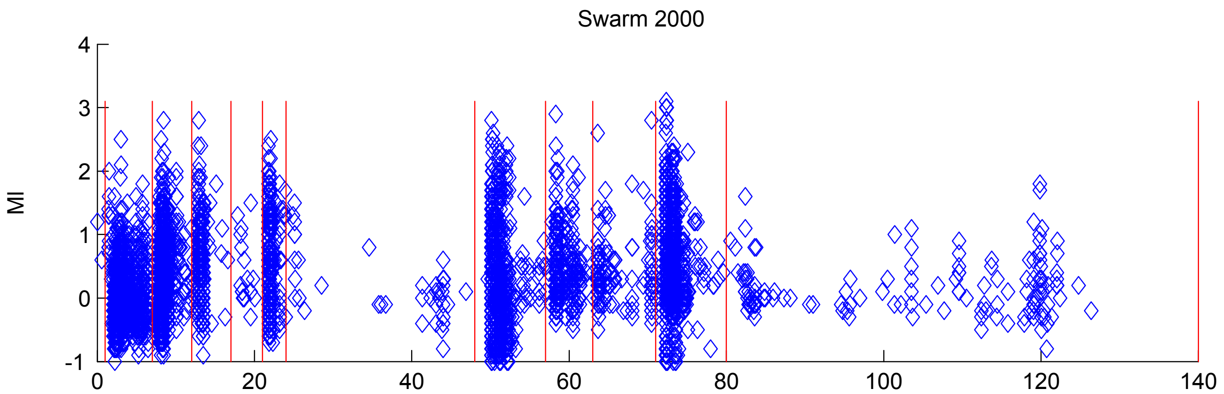

Fig. 8c

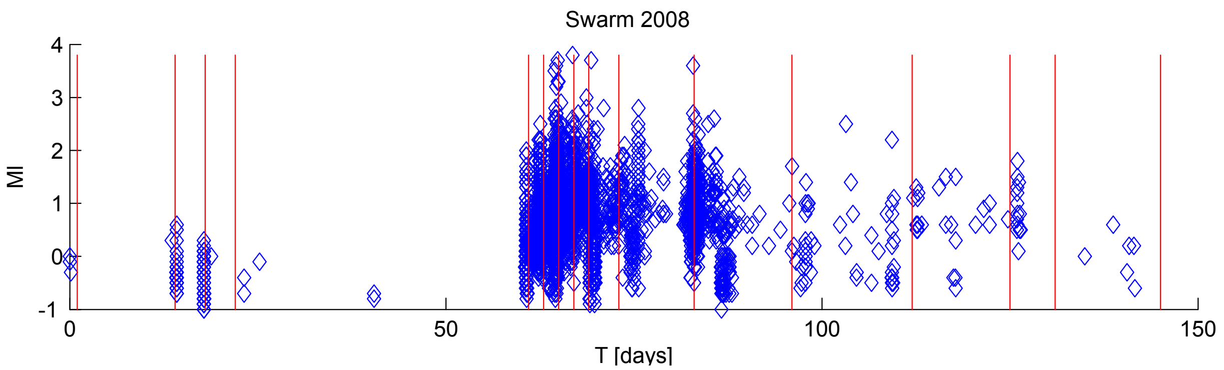

Fig. 8d

Fig. 8 The same time division of the swarms as in Figure 7, but magnitude Ml of investigated events is plotted instead of daily number of events.

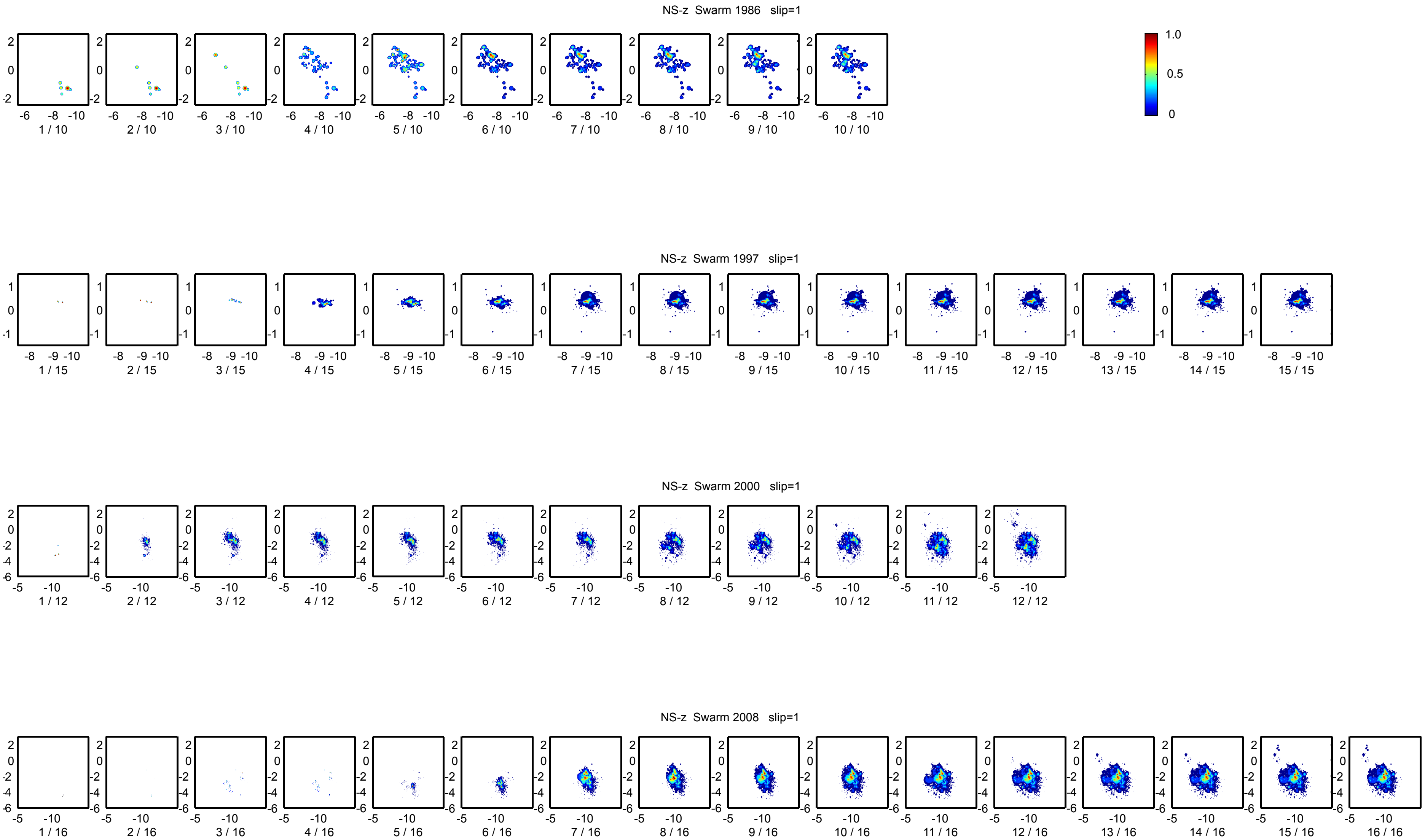

Fig. 9 Time development of slip during the swarms – constant slip model. There are plotted vertical planes oriented in NS direction for time intervals displayed in Figure 7. The distances are given in [km] from Nový Kostel (NKC) station, values of normalized cumulative slip are given in each subplot. The colour or grey scale, respectively, is valid for each subplot. Fig. 9a – 1986; Fig. 9b – 1997; Fig. 9c - 2000 and Fig. 9d - 2008.

on the applied slip model. For constant slip there were observed 2-3 asperities. For the scaled-slip model (eq. 3) the influence of the strongest event become predominant, which arises from the exponential form of slip scaling equation (3), which emphasized the strongest event. There is no indication how to select which slip model should be preferred. However, the patterns obtained for constant slip are more similar to the slip pattern of large earthquakes, e.g. on San Andreas fault (Luis et al., 2008). Such a model corresponds better with our understanding of a swarm as a one (slow) meta-earthquake.

From the temporal-spatial slip patterns it follows, that each of observed swarm can be characterized by three phases:

1. Starting phase with random migration of small events.
2. Main phase containing events where the most energy is radiated, maximal slip in two or three dominated asperities is generated. Prevailing upwards direction of activity migration is observed. This fact supports the hypothesis of triggering the swarm by upward movement of fluids – Horálek and Fischer (2008).
3. Fading phase – with small activity on the swarm touched area – we can speculate about relaxation of small barriers created and/or skipped by previous bigger events.

The estimation of maximal possible displacements indicated that they can reach in the most slipped places orders of meters – particular values are given in Table 1.

The dynamics of the WB swarm seismicity has been discussed in several papers (namely for swarm 2000) – e.g., Fischer and Horálek (2005), Hainzl (2004), Fischer and Horálek (2003), Fischer and Horálek (2000), Hainzl and Ogata (2005). However no quantitative and testable model has yet been launched. We expect that whatever future model of swarm behaviour will be similar to our observed slip patterns. Hainzl and Ogata (2005) suggest that the fluids play important role only at a swarm starting process. It remains an open question, whether lately dominant stress triggering (ibid.) can satisfactory explain observed general upwards migration of the activity.

From general point of view, the obtained images of temporal-spatial swarm activity show that the very detailed swarm development is probably controlled by subtle small local changes of the medium properties, fluid pressure fluctuation and small-scale geometry of the faults. The swarms behaviour then appear to be partly stochastic. And we can finally conclude with a “philosophic” question if it is possible to describe or even predict detailed swarm behaviour in a fully deterministic way.

ACKNOWLEDGEMENT

The work was supported by the grant IAA300120805 of the Grant Agency of Acad. of Sci. of the Czech Republic. The paper finalising was supported by grant P210/10/1728 of the Grant Agency of the Czech Republic. Maps were prepared using the GMT software (Wessel and Smith, 1991).

We are thankful to two anonymous reviewers for improving comments and detailed revision of the text.

REFERENCES

ASPERITIES: 2010, http://www.ig.cas.cz/kolar/StopPhase/Asperity/Asperity.html access: 06 April 2011.

Epicentre map: 2010, http://www.ig.cas.cz/cz/struktura/observatore/webnet/mapa-ohnisek/ access: 25 March 2010.

Fischer, T., and Horálek, J.: 2000, Refined Locations of The Swarm Earthquakes In The Nový Kostel Focal Zone and Spatial Distribution of The January 1997 Swarm In Western Bohemia, Czech Republic, Studia Geophys. et Geodet.. 44, 3, 210–226.

Fischer, T., and Horálek, J.: 2003, Space-time distribution of earthquakes swarms in the principal focal zone of the NW Bohemia/Vogtland seismoactive region: period 1985-2001. J. Geodyn., 35, 125–144.

Fischer, T., and Horálek, J.: 2005, Slip-generated patterns of swarm microearthquakes from West Bohemia/Vogtland (central Europe): Evidence of their triggering mechanism? J. Geophys. Res., 110, B05S0X, DOI:10.1029/2004JB003363.

Imanishi, K. and Takeo, M.: 1998, Estimates of fault dimensions for small earthquakes using stopping phases. Geophys. J. Let., 25, 15, 287–2900.

Imanishi, K. and Takeo, M.: 2002, An inversion method to analyze rupture process of small earthquakes using stopping phases. J. Geophys. Res., 107, B3.

Hainzl, S.: 2004, Seismicity patterns of earthquake swarms due to fluid intrusion and stress triggering. Geophys. J. Int.. 159, Issue 3, 1090-1096. DOI: 10.1111/j.1365-246X.2004.02463.x.

Hainzl, S., and Fischer, T.: 2002, Indications for a successively triggered rupture growth underlying the 2000 earthquake swarm in Vogtland/NW Bohemia, J. Geophys. Res., 107, B12, 2338, DOI:10.1029/2002JB001865.

Hainzl, S., and Ogata, Y.: 2005, Detecting fluid signals in seismicity data throught statistical earthquake modelling. J. Geophys. Res., 110, B05S07, DOI:10.1029/2004JB003247.

Hanks, T.,C. and Kanamori, H.: 1979, A moment magnitude scale. J. Geophys. Res., 84, 2348–2350.

Horálek, J., Fischer, T., Boušková, A., and Jedlička, P.: 2000a, The Western Bohemia/Vogtland Region in the Light of the Webnet Network, Geophys. et Geodet., 44, 2, 107–125.

Horálek, J., Šílený J., Fischer, T., Slancová A. and Boušková A.: 2000b, Scenario of the January 1997 West Bohemia Earthquake Swarm. Geophys. et Geodet., 44, 4, 491–521.

Horálek J. and Fischer, T.: 2008, Role of crustal fluids in triggering the West Bohemia/Vogtland earthquake swarms: Just what we know (a review). Studia Geophys. et Geodet., 52, 4, 661–672.

Keilis-Borok, V. I.: 1959, On estimation of the displacement in an earthquake and source dimension. Ann. Geofis. (Rome), 12, 205–214.

Kolář, P.: 2011, West Bohemia swarm finite circular seismic source model inferred from stopping phases, submitted to Acta Gepohys. et Geodet.

Kolář, P. and Vavryčuk, V.: 1990, Reinterpretation of selected events of West Bohemia swarm 1985/86 (in Czech), internal report of Geophysical Institute.

Luis, A.D., Hiroe, M., Steven, M.D. and Kojiro, I.: 2008, Surface rupturing and buried dynamic-rupture models calibrated with statistical observations of past earthquakes. Bull. Seism. Soc. Am., 98, 3,1147–1161.

Neunhöfer, H.: 1988, Das Bulletin der lokalen Erdbeben im Vogtland 1962 - 1997 (Bulletin of the Vogtland/Western Bohemia earthquakes). DGG Mitteilungen, 4, 2–7.

Studia Geohpysica et Geodetica: 2000, (special issue devotes to West Bohemia topics). 44, 2–3.

Studia Geohpysica et Geodetica: 2008, (special issue devotes to West Bohemia topics – Part 1). 52, 4.

Studia Geohpysica et Geodetica: 2009, (special issue devotes to West Bohemia topics – Part 2). 53, 3.

Vavryčuk, V.: 2011, Principal earthquakes: Theory and observations from the 2008 West Bohemia swarm, Earth Planet. Sci. Lett., in press, DOI:10.1016/j.epsl.2011.03.002.

Wessel, P. and Smith, W.H.F.: 1991, Free software helps map and display data. EOS Trans. AGU, 441, 72.

wwwWEBNET: 2010, http://www.ig.cas.cz/en/structure/observatories/west-bohemia-seismic-network-webnet/ access: 25 October 2010.

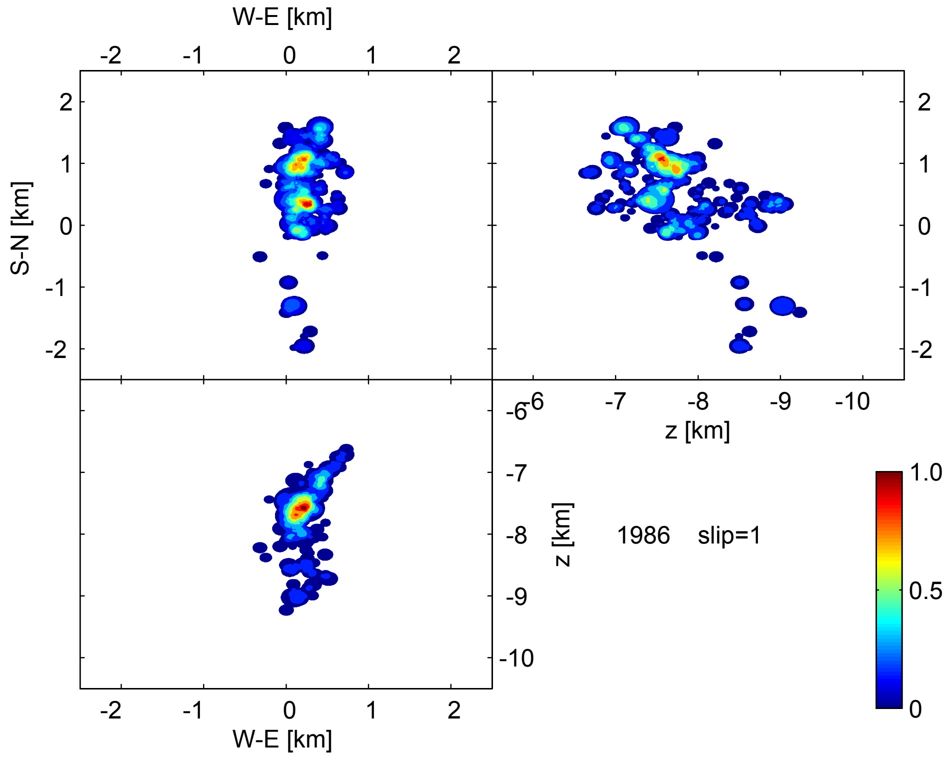

Fig. 3a

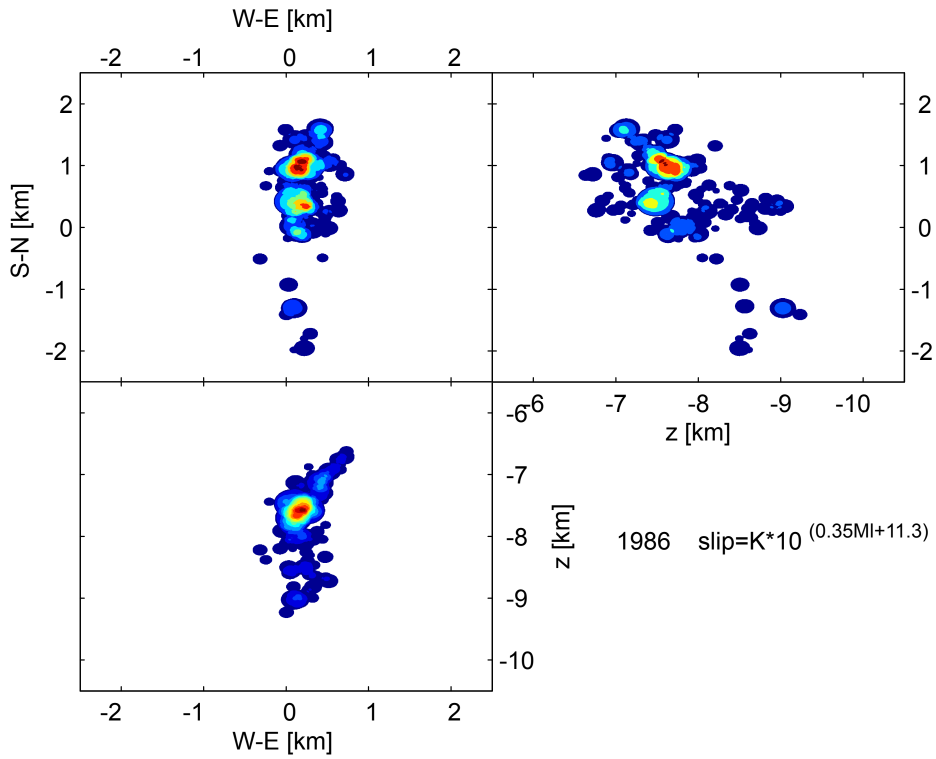

Fig. 3b

Fig. 3 Final slip of swarm1986; horizontal projection (in NS-EW orientation) – upper left part; vertical projection into NS-z plane, view from E – upper right part; vertical projection in EW-z plane, view from S - lower left part. Distances are given in [km]; origin is in station Nový Kostel (NKC, N50.2331 E12.4479, alt. 564m). The asperities situated on one plane oriented in NS direction, with decay to W at the bottom can be seen. Value of slip are normalised individually for each projection; colour scale is valid for all successive figures of the slip projections (Figs. 4-6). The uncorrupted area is left uncoloured or white respectively.
3a) constant slip model.
3b) scaled slip model.

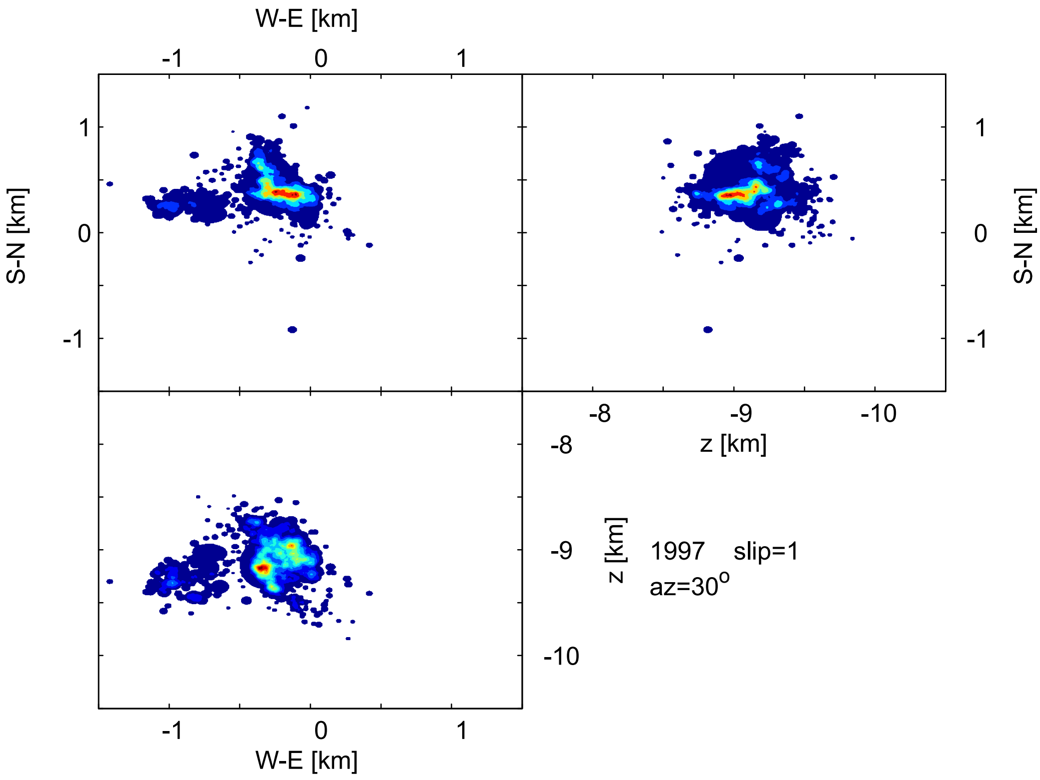

Fig. 4a

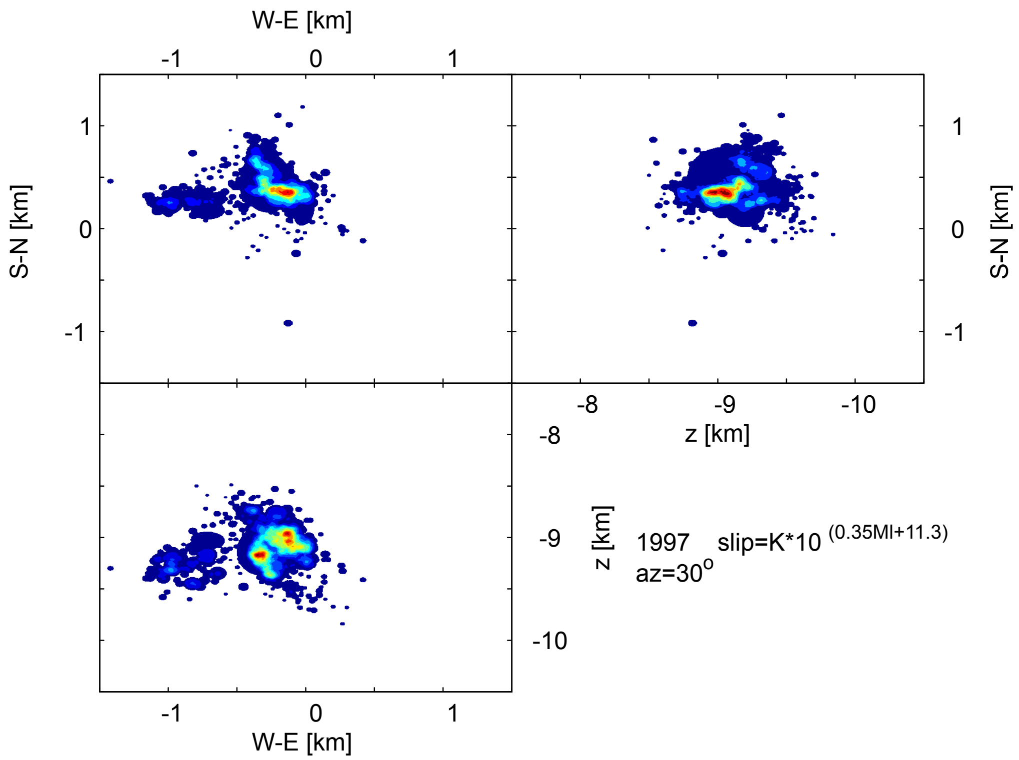

Fig. 4b

Fig. 4 Final slip of swarm 1997 (the same projection as in Figure 3), horizontal coordinates rotated by 30° clockwise. Note, that swarm 1997 has affected smaller area than other investigated swarms.
4a – constant slip model; two principal asperities on two perpendicular planes can be identified.
4b – scaled slip model; here the subtle fault geometry is "lost" and only one asperity prevails.

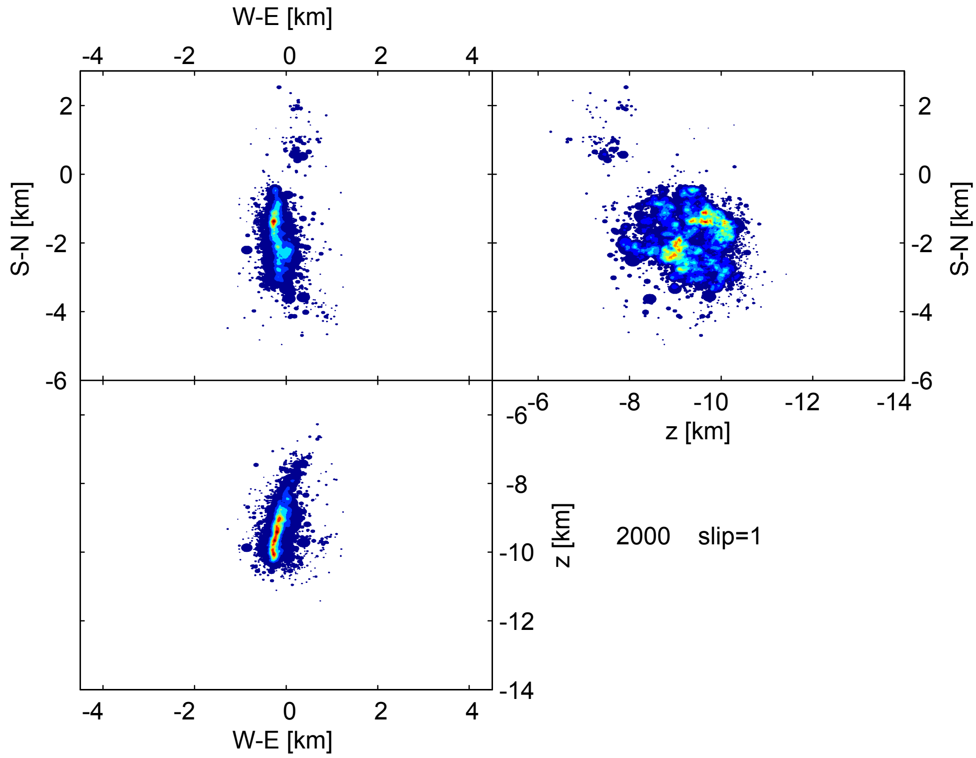

Fig. 5a

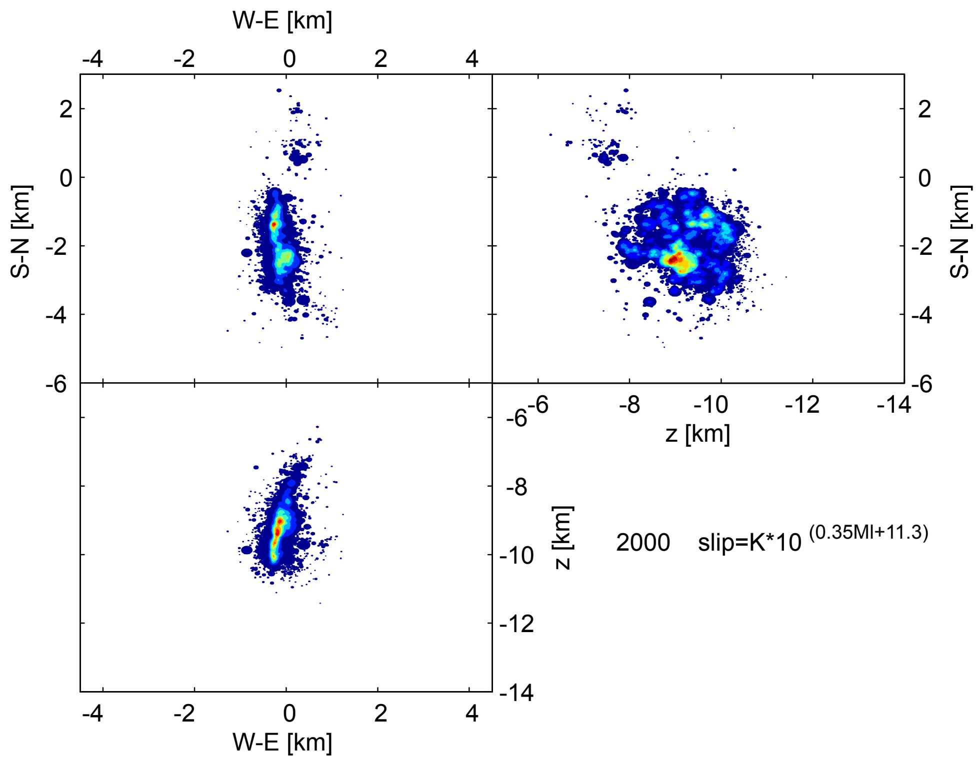

Fig. 5b

Fig. 5 Final slip of swarm 2000 (the same projection as in Figure 3). Two to three principal asperities laying on one sub-vertical plane oriented approximately in NS direction can be seen – in this case there is no such big difference between two slip models.
5a – constant slip model.
5b – scaled slip model.

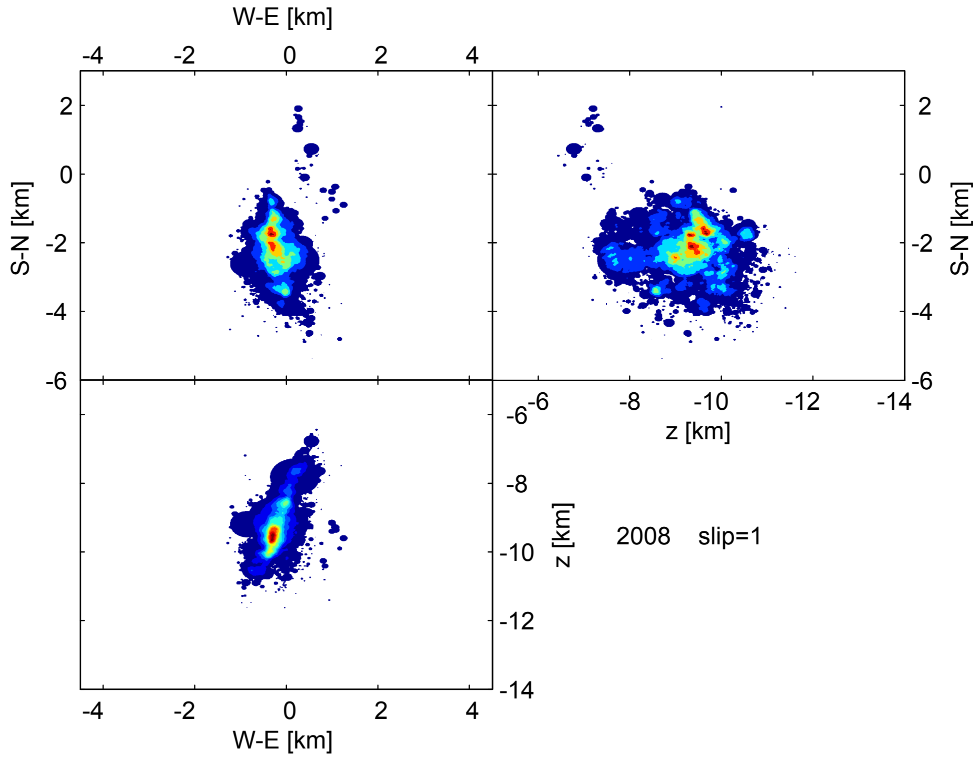

Fig. 6a

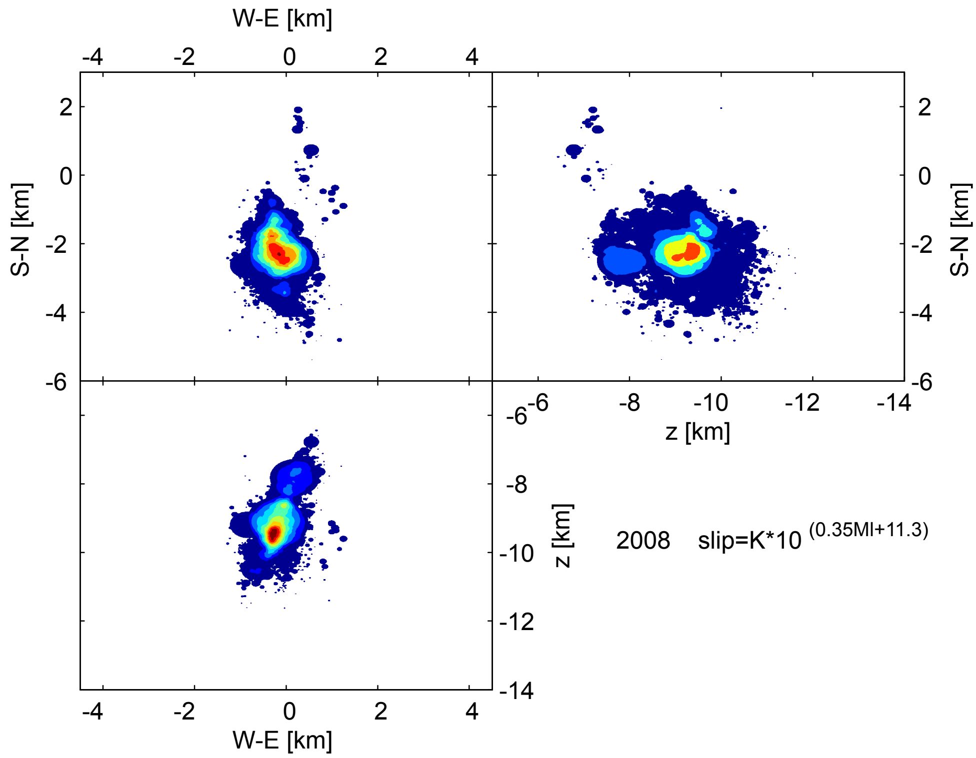

Fig. 6b

Fig. 6 Final slip of swarm 2008 (the same projection as in Figure 3).
6a – constant slip model.
6b – scaled slip model. Here, main asperities again prevail, however the others can still be seen.